Activity report of experiment LS-3136 on ESRF Beamline ID16A

A) Subcellular distribution and stability studies of organometallic gold(III) complexes by cryo-correlative light-XRF microscopy

Context of the experiment

In a study carried out in our laboratory, we demonstrated that organometallic gold(III) complexes bearing (N^N)-type bipyridine or phenanthroline chelating ligands displayed anticancer activity on cell cultures. However, when incubated with stoichiometric amounts of histidine or cysteine for 24 h at 37 °C, quantitative substitution of the (N^N) chelate was observed. Therefore, replacement of the (N^N) chelate was decided. We chose to exchange (N^N) chelates by more donor diphosphine ligands (P^P). The same stability experiments in the presence of histidine and cysteine were conducted. In the case of the (P^P)-containing complexes, no reaction with histidine and cysteine was observed and the native complexes were preserved. Similarly, no reaction was observed upon incubation of the complexes with up to 50 eq. of glutathione (GSH) a tripeptide present at a millimolar concentration in intracellular environment and responsible for metal-based complexes detoxification, after 24 h at 37 °C.

Nevertheless, the following questions raised: 1) Is the structure of the (P^P)-containing complexes maintained within the cancer cells ? Do the complexes accumulate in particular regions of the cells and if yes, where ?

To answer these questions, we applied for beam time at the ESRF beamline ID16A. We analyzed lung cancer cells A549 treated with a (P^P)-containing complex presenting a bromine atom on the (P^P) chelate. Thus by measuring the quantity and the localization of both Au and Br within the cell, we will be able to assess the integrity or not of the complexes. Moreover by correlating cryo-fluorescence microscopy using organelle-specific fluorescent dyes with the XRF maps of Au we will be able to determine the intracellular localization of the complexes. As controls we used cells treated with a gold complex comprising a Br-labelled (N^N) chelate and untreated cells.

Intracellular integrity of the (P^P)-based complex

A549 cells deposited on graphene-coated Si_3N_4 membranes were incubated with 1 µM of complex for 4 h followed by organelles labelling (Hoechst 33342 for nucleus, Mitotracker Green for mitochondria and Lysotracker Red for lysosomes).

The complete membrane was imaged using cryo-fluorescence microscope. We then selected three representative cells for XRF microscopy analysis. Images depicting the distribution of characteristic endogenous elements as well as gold and bromine are showed in figure 1 together with the fluorescence image recorded on the same field (3 channels).

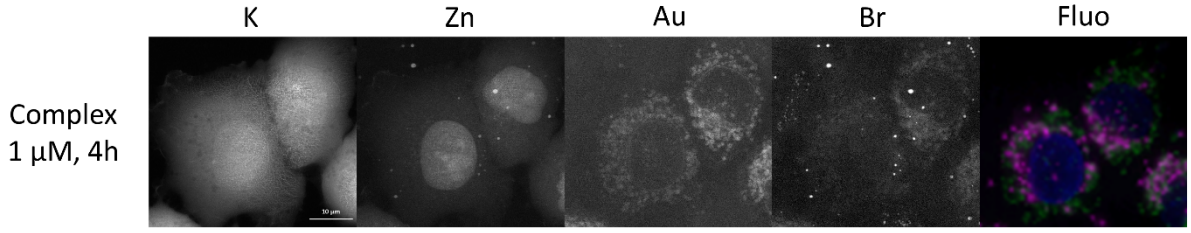

Figure 1 : XRF images of A549 cells treated with a Br-labelled (P^P)-based organometallic gold(III) complex. Fluorescence image of the same cells co-stained by Hoechst, Mitotracker green and Lysotracker Red (lysosomes in pink, nucleus in blue, mitochondria in green).

We could clearly observe the presence of both Au and Br inside the cells with an identical pattern, suggesting indeed colocalization of Au and Br. We measured the quantity of Au and Br inside the three

studied cells and both elements appeared to be in a 1/1 ratio, in agreement with the molecular structure of the complex (figure 2A). To gain information on the spatial colocalization, we measured at each pixel the quantity of Au and Br along a line (figure 2B) and we could observe that the quantity of Au and Br were identical at each point (figure 2C). Altogether, these data confirm the intracellular integrity of the (P^P)-containing complex.

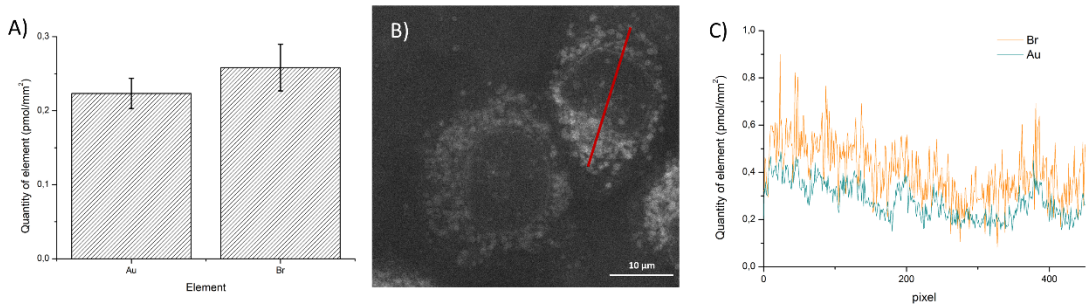

Figure 2 : A) Intracellular Au and Br concentrations measured in three independent cells. B) Measurement (red line in upper cell) of local Au and Br quantities. C) Au and Br concentrations along the red line shown in B.

Intracellular localization of the (P^P)-based gold complex

We recorded four images at the highest resolution on small areas of a cell and superimposed the obtained XRF Au maps and the cryo-fluorescence image of the same cell. The Au-containing areas appeared to colocalize with the Mitotracker green-labelled areas, suggesting mitochondrial accumulation of the complex (figures 3 and 4). As for the colocalization between Au and Br, we measured for each area the Au quantity and the Mitotracker Green fluorescence intensity. After normalization of the curves, we could observe very similar evolution of both signals, suggesting that the (P^P)-based complex is preferentially accumulated inside the mitochondria.

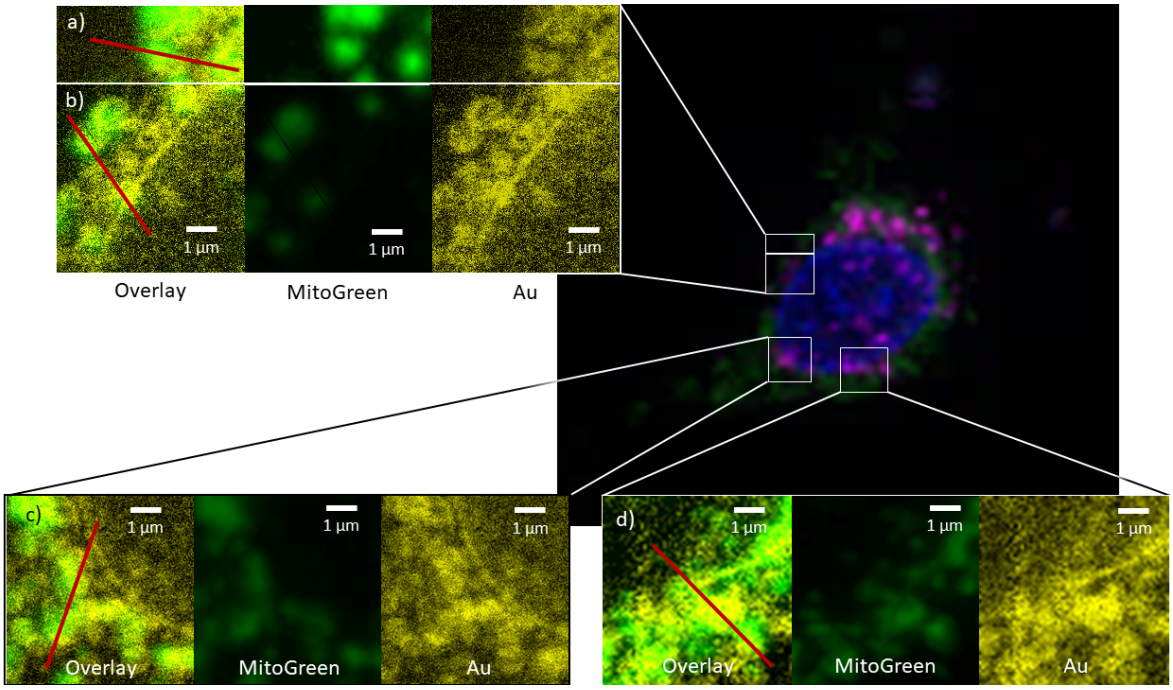

Figure 3 : Fluorescence imaging of a cancer cell and the different areas observed by XRF. For each area, the XRF Au map, the Mitotracker Green map and the overlay are presented.

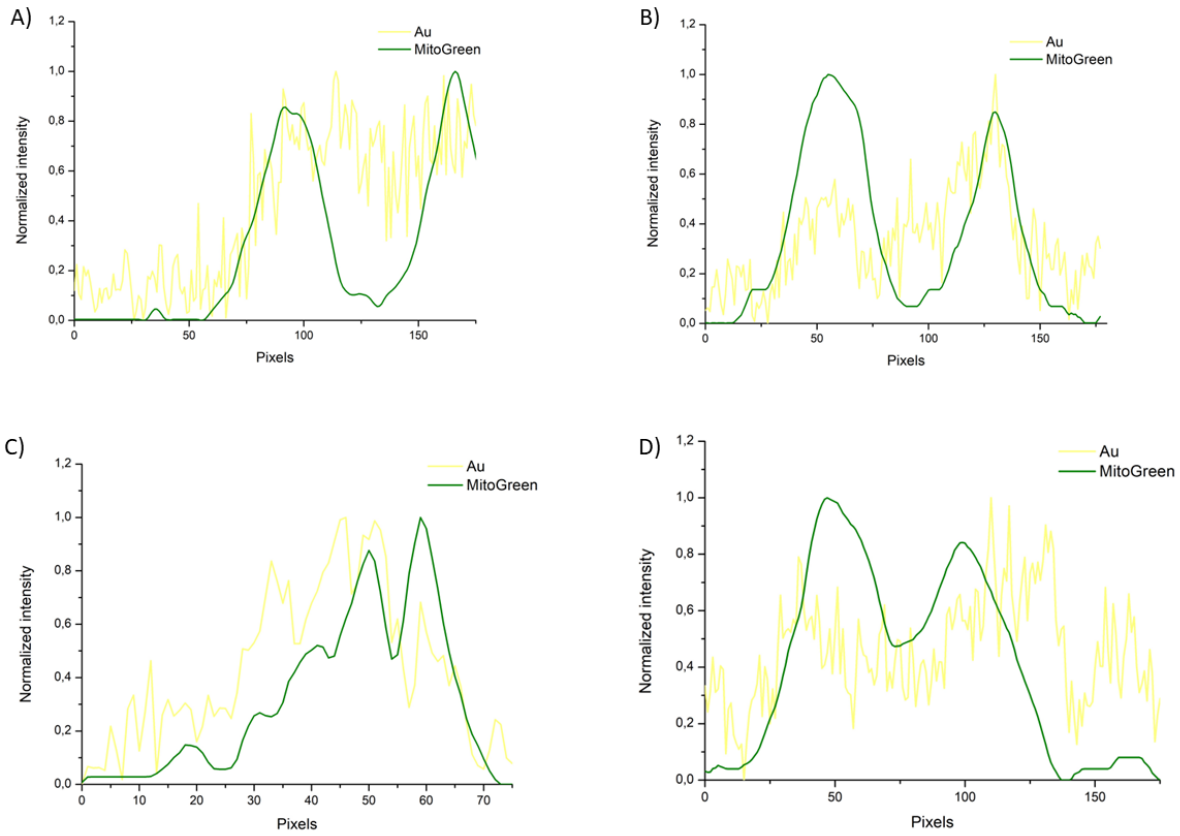

Figure 4 : Spatial evolution of Au quantity and Mitotracker Green intensity after signal normalization recorded for a-d areas in figure 3.

These data prompted us to compare the cryo-fluorescence images obtained for the treated and non-treated cells. In both samples, we measured the Mitotracker Green and Lysotracker Red fluorescence intensities for 25 different cells (figure 5). These data clearly show a reduction of the Mitotracker Green fluorescence intensity in the treated cells while the Lysotracker Red intensity was kept constant suggesting, that the (P^P)-based complex may have induced mitochondrial damages in the A549 lung cancer cells.

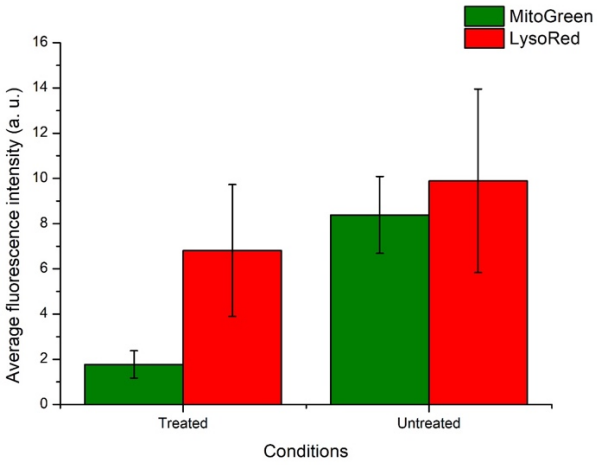

Figure 5 : Mitotracker Green and Lysotracker Red fluorescence intensities measured for 25 (P^P)-based gold complex-treated and untreated cells.

XRF mapping of A549 cells treated with Br-containing (N^N)-based gold complex

As a control we analyzed by XRF microscopy 3 cells treated with 1 µM of a Br-containing (N^N)-based gold complex. This complex is 10 times less toxic than the (P^P)-based complex on the selected cancer cell line and, at the studied concentration, neither Au nor Br could be detected within the cells, suggesting that the difference in activity between both complexes might be due to a reduced intracellular accumulation of the (N^N)-based gold complex with respect to the (P^P)-based one.

XRF mapping of untreated A549 cells

As control, XRF maps of one untreated cell were recorded. As expected, no gold was present in untreated cells and only a small amount of bromine was present (figure 6). This natural bromine comes from the cell culture medium. The other endogenous elements K and Zn give information on the cell morphology (K) and localization of nucleus (Zn).

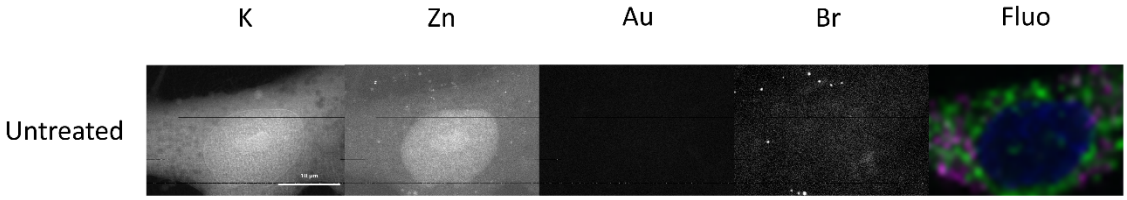

Figure 6 : XRF maps of an untreated A549 cell

Conclusions

Experiment LS-3136 enabled the first example of intracellular speciation of a gold(III) complex in cancer cells. The integrity of the (P^P)-based gold complex could be unambiguously established. We could also demonstrate its accumulation in mitochondria and the probable induction of mitochondrial damages after exposure to 1 µM complex for 4 h. Based on these results, biological studies are ongoing to confirm the mitochondrial damages and explore the potential targets of this complex. These results will appear in a PhD thesis that should be defended in autumn 2023 and in a publication expected in late 2023 or beginning of 2024.

B) <u>Subcellular distribution of a half-sandwich iridium(III) complex by cryo-correlative light / XRF microscopy</u>

Context of the experiment

In the laboratory, we have also developed an array of organometallic iridium(III) complexes comprising (C^N) phenyloxazoline chelating ligands whose antiproliferative properties were demonstrated on various cancer cell lines. From this series of complexes, Ir2 was selected as our lead compound on which comprehensive biological studies were further performed to understand its mechanism of action. As an addition to these studies, we also performed fluorescence imaging experiments with an iridium derivative carrying a fluorescent BODIPY entity. Although we could precisely delineate the subcellular distribution of this complex, we anticipate that the presence of the BODIPY entity may not reflect the localization of Ir2. XRF microscopy with the ID16A beamline offers the possibility to determine with high spatial resolution the distribution of Ir in cells close that their native state without the necessity to label the complex.

Intracellular localization of the iridium complex Ir2 in hTERT-RPE1 cells

hTERT-RPE1 cells were deposited on graphene-coated Si_3N_4 membranes previously treated with fibronectin and let to adhere for 4 h at 37°C under 5% CO_2. Cells were stained with SPY650-FastAct (actin fluorescent dye) for 90 min including 30 min of co-staining with Mitotracker Green and Hoechst

33342. After washing, cells were treated with a 5 µM solution of Ir2 in complete medium for 15 min, washed with ammonium acetate and plunge-frozen in liquid ethane. Cells only exposed to complete medium were prepared for control. The entirety of the membranes was imaged using cryo-fluorescence microscope (3 channels). Cells selected according to their shape and the morphology of their intracellular compartments were imaged by XRF microscopy. Figure 7 shows the fluorescence images of a hTERT-RPE1 cell and the K, P, Ca, Zn and Ir maps of the same cell established by XRF microscopy.

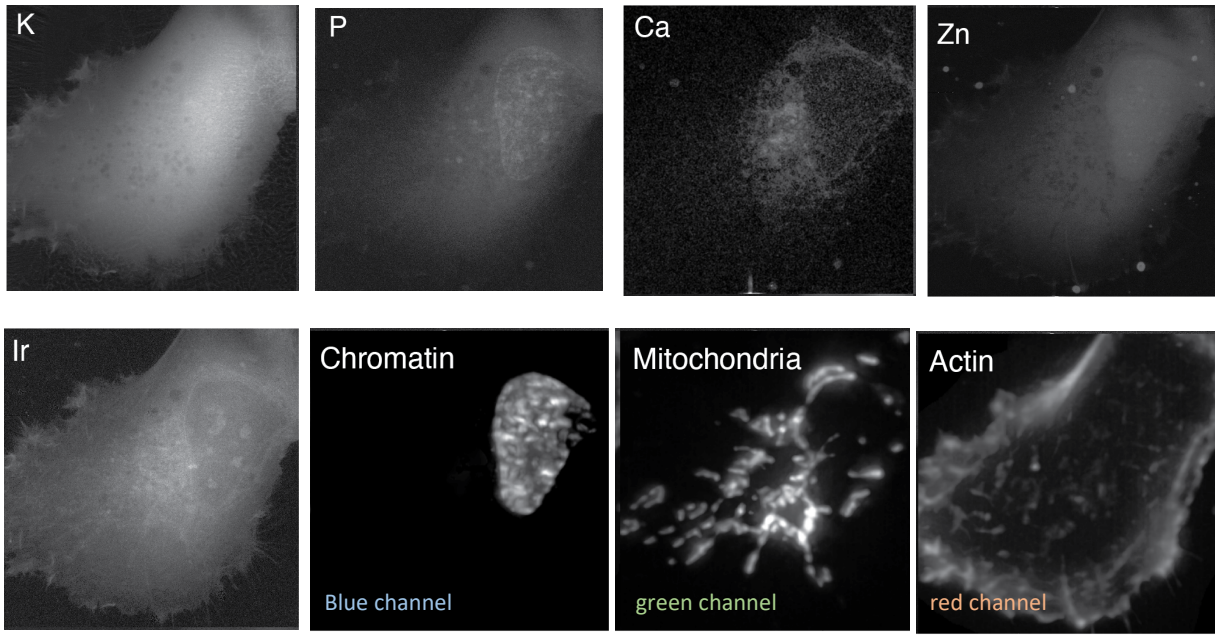

Figure 7. Top: Elemental distribution of endogenous elements in a hTERT-RPE1 cell by XRF microscopy acquired at 50 nm/px/50 ms resolution; Bottom, left: Ir map of the same cell acquired at the same resolution; right: Fluorescence microscopy images of the same cell stained by SPY650-FastAct, (actin network), Mitotracker Green (mitochondria) and Hoechst 33342 (nucleus)

XRF microscopy analysis revealed that Ir can be readily detected in the cytoplasm and the nucleus and appeared enriched in structures identified as mitochondria, actin bundles and the nuclear envelope thanks to cryo-optical fluorescence microscopy. Localization in the actin network and mitochondria was confirmed by recording data at the highest resolution of ID16A (figure 8.)

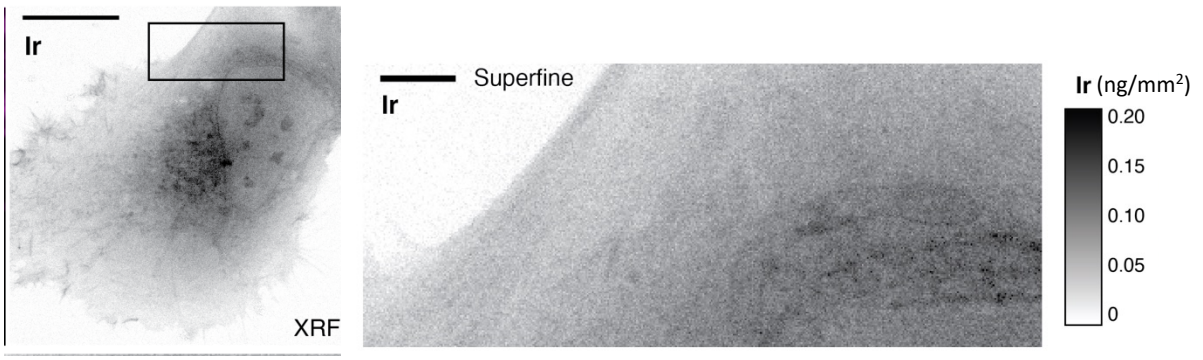

Figure 8. Left: XRF Ir map hTERT-RPE1 cell acquired at 50 nm/px/50 ms resolution; Right: zoom on the region delimited by the square acquired at "superfine" resolution (30 nm/px/100 ms)

XRF mapping of an untreated cell

For comparison, an untreated hTERT-RPE1 cell was also mapped by XRF microscopy (figure 9).

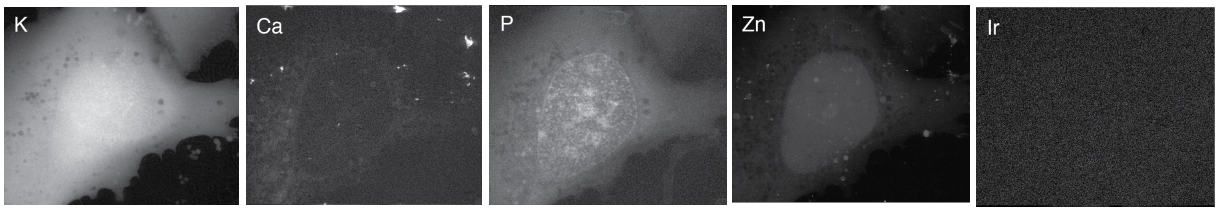

Figure 9. Elemental distribution of endogenous elements and Ir in an untreated hTERT-RPE1 cell acquired at 50 nm/px/50 ms resolution

As expected, no iridium was detected and the distribution of endogenous elements was fully compliant.

Conclusions

Experiment LS-3136 enabled to reliably establish the distribution of the anticancer metallodrug candidate Ir2 in cells under close to native conditions (frozen hydrated). The exceptional resolution reached with the ESRF ID16A nanoprobe and the ability to perform correlative measurements with light microscopy provides a unique environment to study the interaction of metal-based compounds with living systems. A manuscript including these results is currently in preparation and will be soon submitted to Nature Chemistry.